DesignCon 2012

A Causal Huray Model for Surface Roughness

J. Eric Bracken, ANSYS Inc.

Abstract

The recently proposed Huray model is very accurate for modeling surface roughness. It can be used to modify the impedance boundary conditions within an electromagnetic field solver but suffers from causality problems when used for time-domain simulation. This paper discusses the reasons for these causality problems, and proposes a modification to the model to ensure that it will produce causal results. The proposal is to replace the real-valued Huray loss factor with a carefully constructed complex-valued function that matches the loss characteristics of the original model, and is provably causal. A simple formula for the resulting surface roughness model will be given, and analysis results will be presented to demonstrate its accuracy and effectiveness.

Author Biography

Eric Bracken is an R&D Fellow with ANSYS Inc. (formerly Ansoft Corp.) in Pittsburgh, PA. He received his B.S., M.S. and Ph.D. degrees in Electrical and Computer Engineering from Carnegie Mellon University. His research interests are in the areas of model order reduction, signal and power integrity, parasitic extraction, circuit theory and circuit simulation.

Introduction

Surface roughness effects are an important consideration for high-speed digital design because they lead to increased losses in interconnects. These added losses cause greater attenuation and dispersion, which can increase bit error rates in data channels on printed circuit boards and packages. Early attempts at surface roughness modeling, such as those by Hammerstad and Jensen [1] or Groiss and Bardi *et al.* [2] used a curve fitting approach: the observed loss increase was fitted with simple analytic functions to the average roughness value of the surface. These models were found to be adequate for surfaces with low to moderate roughness. Recently Huray et al. proposed a physics-based "snowball" model for surface roughness [3]. Their model is based upon analytic solutions for the fields surrounding a hemispherical ball attached to a metal surface. The Huray model has been found to be more accurate than earlier approaches when the surface is very rough (as it is in many copper foils used in the manufacture of modern printed circuit boards.)

2D and 3D electromagnetic solvers typically use some form of impedance boundary condition (IBC) to model the field behavior on metal surfaces. It is natural to attempt to treat the surface roughness model as a modification to the IBC. The most straightforward approach is to use the loss increase from the roughness model as an additional multiplying factor. This yields good results in the frequency domain. Unfortunately, this approach leads to problems if the frequency domain results are used as a starting point for time-domain simulation. The problem is that the real-valued loss factor gives rise to non-causality in the impedance function for the IBC. This non-causality then leads to problems if we attempt to perform simulations in the time domain.

In this paper, we will discuss the reasons for this non-causal behavior. Then we will describe an alternative approach to address the problem. The proposal is to construct a complex-valued loss factor that exactly reproduces the predicted losses from the real-valued Huray model, and to do this in a way that is provably causal in the time domain. A simple formula for this complex loss factor will be given. Using 3D field solver experiments, we will present some numerical results using this causal version of the Huray model to demonstrate its accuracy and effectiveness.

Impedance Boundary Conditions

An impedance boundary condition or IBC is a relationship between the current density J and the electric field E on the outer surface of a conductor. It is characterized by an equation of the form

$$E = Z_s(j\omega)J \tag{1}$$

Here Z_s is the surface impedance, with units of Ohms. It is a function of angular frequency $\omega = 2\pi f$, where f is the frequency measured in Hertz. The symbol $j = \sqrt{-1}$ is used for the imaginary unit. The IBC is convenient in a field solver because it allows one to treat the interior of good conductors as a field free region, thus avoiding a great deal of computational expense for meshing inside the conductor.

The surface impedance is often derived in textbooks by assuming a flat conducting object that is semi-infinite in thickness, with conductivity σ and magnetic permeability μ. The resulting expression for Z_s is

$$Z_s(j\omega) = \sqrt{\frac{j\omega\mu}{\sigma}} \tag{2}$$

Associated with the surface impedance is a quantity known as the skin depth, the effective depth of penetration of the electric and magnetic fields into the conductor. The skin depth $\delta(\omega)$ is

$$\delta(\omega) = \frac{1}{\sqrt{\pi f \mu \sigma}} \tag{3}$$

The textbook form of the surface impedance suffers from a practical limitation: as frequency $\omega \to 0$, $Z_s \to 0$ as well, leading to a perfect, zero-resistance conductor at DC. The problem here is that the skin depth in this idealized model has been allowed to grow infinitely large at low frequencies. To address this issue, it is possible to take into account the finite thickness h of the conductor in the derivation of the IBC. The resulting surface impedance is then finite at low frequency. An expression for the finite-thickness surface impedance Z_s^{FT} derived by this approach is

$$Z_s^{FT}(j\omega) = Z_s(j\omega)\coth(h\sqrt{j\omega\mu\sigma}) \tag{4}$$

This has the correct DC limit $Z_s^{FT} \to 1/(\sigma h)$. At high frequencies (where the skin depth is small compared to the conductor thickness) the coth() function becomes 1, and the two formulas become indistinguishable: $Z_s^{FT} \to Z_s$.

Surface Roughness Effects

In reality, no conductor has a perfectly flat surface. Sometimes the metal may even be roughened deliberately during manufacturing to improve the adhesion between layers in a printed circuit board. Chemical roughening leads to a large collection of copper dendrites on the metal surface. A typical copper foil appearance resulting from such a roughening process is shown in the figure below:

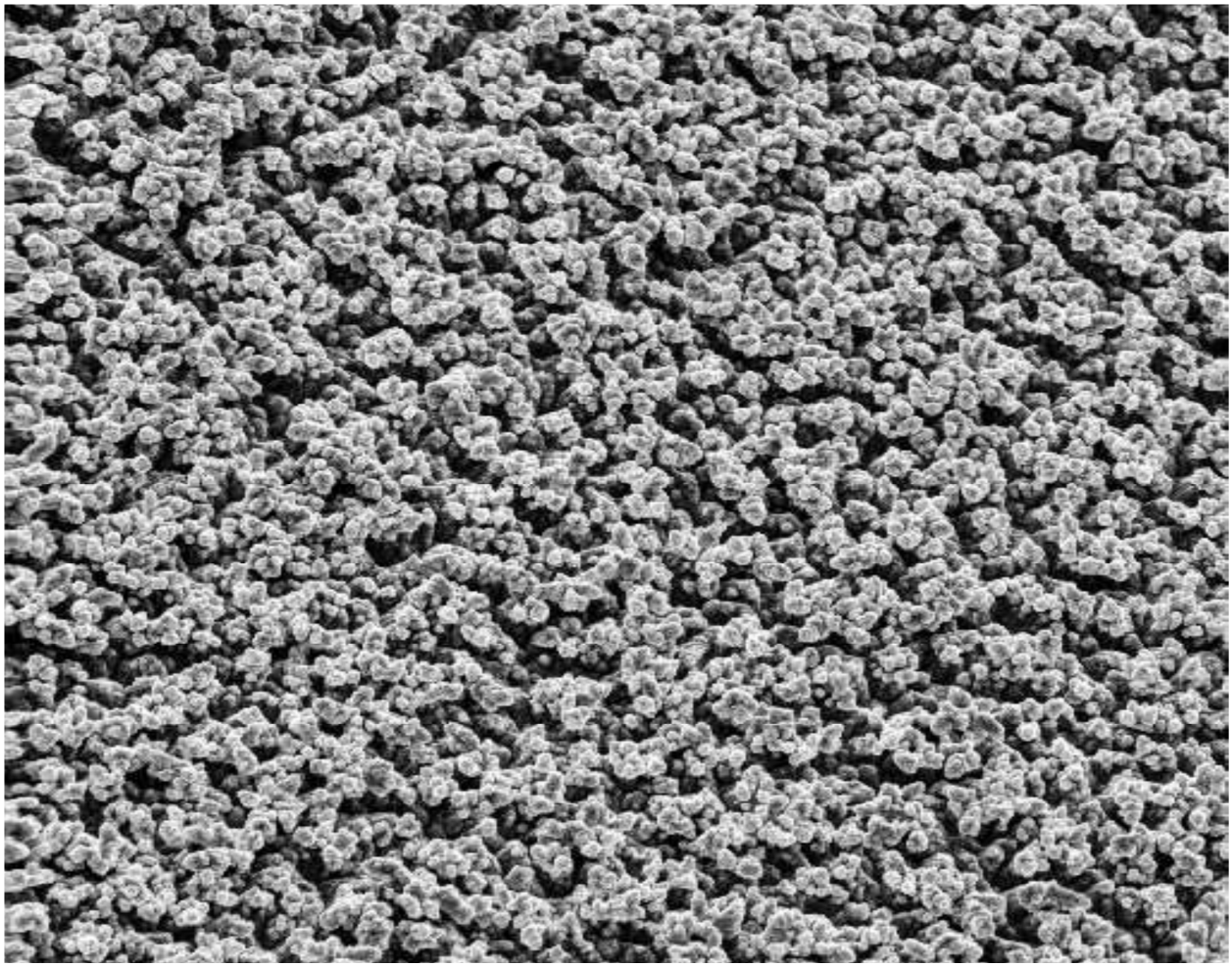

Figure 1. Scanning electron microscope photograph of a roughened copper foil surface.

The large increase in the metal surface area relative to a smooth surface will certainly have an effect on current transport, increasing the observed loss. This is particularly true when the skin depth is comparable to or less than the average height of the surface protrusions. Typical mean heights for these surfaces are in the range of 0.5 to 6 microns. The skin depth in copper at 1 GHz is about 2 microns, so roughness effects will be prominent for multi-gigahertz signal components.

The purpose of this paper is not to explore the detailed physics of rough surfaces. The interested reader is referred to the papers by Huray et al. [3] [4] for more details. Briefly, the procedure adopted there is to use a first-principles electromagnetic analysis to determine how a plane wave scatters from or is absorbed by a spherical conductor. The result of this analysis is an analytic expression for the loss as a function of various parameters such as the sphere's radius, the frequency, metal conductivity, etc.

As can be seen from Figure 1, the actual rough surface is considerably more complicated than a single isolated hemisphere. There is a random, densely packed arrangement of roughly spherical

nodules piled atop one another and they are not all of a single, uniform size. Therefore some approximations need to be made to extend the analysis from a single sphere to the actual surface. Huray et al. in [4] have done this and give some explanations for why their approximations work. (They also provide a comparison of this model's predictions with measured data from microstrip traces built on low- and high-roughness metal foils, and the agreement is very good.) They ultimately arrive at the following analytic model for a rough surface:

$$H_r(j\omega) = \frac{P_{rough}}{P_{smooth}} = 1 + \frac{3}{2}\sum_{i=1}^{n} \frac{N_i 4\pi a_i^2}{A_{hex}} \cdot \left[1 + \frac{\delta}{a_i} + \frac{\delta^2}{2a_i^2}\right]^{-1} \tag{5}$$

Here P_{rough} denotes the power loss for a section of rough surface of area A_{hex}, and P_{smooth} is the power loss for an ideal smooth surface of the same area. The model allows for the possibility of n different classes of spherical nodules. Within in each area A_{hex} it assumes that there are N_i spheres of radius a_i, for each class $i = 1, \cdots, n$. Finally the quantity δ denotes the skin depth from (3). It is through the skin depth that (5) becomes a function of frequency.

Eq. (5) can be used to obtain the power losses for a rough surface if the losses for a smooth surface are known. We return now to our IBC for the smooth surface as given in (2). The surface impedance has real and imaginary parts:

$$Z_s(j\omega) = R_s(j\omega) + j\omega L_s(j\omega) = \sqrt{\frac{\omega\mu}{2\sigma}} + j\sqrt{\frac{\omega\mu}{2\sigma}} \tag{6}$$

Here we have used the identity $(1 + j)^2 = 2j$. We identify the real part with the surface "resistance" $R_s(j\omega)$ and the imaginary part with the inductance $L_s(j\omega)$. Recall from basic circuit theory that the resistance part will control the power losses: $P_{smooth} = \frac{1}{2}R_s|J|^2$. The increase in power loss due to (5) therefore points to an increase in the effective surface resistance:

$$R_{rough}(j\omega) = H_r(j\omega) \cdot R_s(j\omega) \tag{7}$$

Eq. (7) seems simple enough to implement—we already know from (5) and (6) what each of the factors on the right hand side should be. Unfortunately, it is here that we begin to run afoul of causality issues. This is the topic of the next section.

Causality Issues

Simply stated, a system is *causal* if it does not produce any change in its output signal before there is a change in its input signal. All known physical systems are causal. For the case of a linear time-invariant system, we can characterize its behavior by an impulse response $h(t)$. If the system is causal, then the impulse response satisfies the condition

$$h(t) = 0 \text{ for } t < 0.$$

Electromagnetic problems are often solved in the frequency domain. The impulse response is then converted to its Fourier transform, $H(j\omega)$. When the above causality condition is translated into the frequency domain it becomes a pair of *Hilbert transform* relations. (Sometimes these are called the Kramers-Krönig relations.) Splitting the complex quantity $H(j\omega)$ into its real and imaginary parts $H(j\omega) = X(j\omega) + jY(j\omega)$, the Hilbert transform relations are

$$X(j\omega) = \frac{1}{\pi} PV \int_{-\infty}^{\infty} \frac{Y(j\xi)}{\xi - \omega} d\xi$$

$$Y(j\omega) = -\frac{1}{\pi} PV \int_{-\infty}^{\infty} \frac{X(j\xi)}{\xi - \omega} d\xi$$

Here the "PV" denotes the Cauchy principal value, a technical way of assigning a value to these integrals. These expressions may appear formidable, but there is a simple interpretation of them: for a causal signal, the real and imaginary parts of its Fourier transform are not independent. Knowing the real part $X(j\omega)$, we can (at least in theory) reconstruct the imaginary part $Y(j\omega)$, and vice versa. Conversely, if we start in the frequency domain, we cannot select arbitrary functions $X(j\omega)$ and $Y(j\omega)$ for the real and imaginary parts of the transfer function if we want to ensure it is causal.

To be even more specific, consider a transfer function that has a frequency-varying real part and zero imaginary part. From the definition of the Fourier transform,

$$H(j\omega) = \int_{-\infty}^{\infty} h(t) \exp(-j\omega t)\, dt = \int_{-\infty}^{\infty} h(t)\cos(\omega t) dt - j \int_{-\infty}^{\infty} h(t)\sin(\omega t) dt$$

The function $\sin(\omega t)$ is odd: $\sin(-\omega t) = -\sin(\omega t)$. Therefore, for the second integral representing the imaginary part to be zero for all values of frequency ω, the impulse response $h(t)$ should be an even function: $h(-t) = h(t)$. But this contradicts the assumption that the signal is causal, because $h(-t)$ should be zero for all $t > 0$. [1] Therefore, we conclude that a transfer function with frequency-varying real part and zero imaginary part is non-causal. In fact it is completely non-causal because the impulse response function $h(t)$ has mirror-image even symmetry.

The smooth surface impedance functions given in (2) and (4) are necessarily causal, because they relate a physical input (current density *J*) to a physical output (tangential electric field *E*). If we now modify the real part alone by multiplying with the Huray rough surface loss factor of (5), we will clearly destroy the Hilbert transform relationship that originally existed between the real and imaginary parts. The resulting surface impedance is then no longer a causal function.

---

[1] The only causal function that can have a Fourier transform with zero imaginary part is one that is zero for almost all time—for example, a Dirac delta function at time $t = 0$. But the Fourier transform of such a function is independent of frequency, and we have excluded this case by assumption.

A more sophisticated approach might be to multiply both the real and imaginary parts of the smooth surface impedance by the Huray factor $H_r(j\omega)$. It is at least possible now to imagine that the Hilbert transform relation may have been preserved. We must now investigate whether this is really the case.

Consider first the fact that the Huray factor in (5) is a real-valued quantity. This follows because all of the quantities in the formula, including the skin depth, are real numbers. Now the skin depth is a frequency-dependent quantity, going as $\omega^{-1/2}$, and so the roughness factor $H_r(j\omega)$ is a real-valued, frequency-dependent quantity. We have already argued that such a real-valued function of frequency cannot represent the transfer function of a causal system.

Now consider the well-known fact from linear system theory that multiplication of two functions in the frequency domain corresponds to convolution of the inverse Fourier transforms of those functions in the time domain [5]. Therefore, the time-domain signal obtained through this process would be the convolution of the impulse response of the smooth surface (a causal function) with the impulse response of the real-valued Huray loss factor (a non-causal function.) The resulting time response will therefore be non-causal as well. We have not yet achieved our desired goal: a physical, causal response for the rough surface.

This causality issue is not merely a theoretical concern. It has serious consequences for time-domain simulation, as discussed in the next section.

Importance of Causality for Time-Domain Simulation

It is often desirable to use the results of an electromagnetic analysis to generate time-domain waveforms. This allows an engineer to study the signal integrity effects of propagation delay, characteristic impedance mismatch, attenuation, dispersion, crosstalk, etc. on parameters of direct interest in a digital system, such as bit error rates. This is most often accomplished by converting the results of a frequency-domain electromagnetic simulator back to the time domain using some form of inverse Fourier transform (followed by numerical convolution) or by fitting a rational function model to the frequency response. Rational function fitting can be done in many ways, but all of them conceptually involve fitting a set of poles and residues to the frequency domain data:

$$H(j\omega) \cong k_0 + \sum_{i=1}^{N} \frac{k_i}{j\omega - p_i} \tag{8}$$

The reader may recall that such a function has an analytic impulse response representation,

$$h(t) = k_0\delta(t) + \sum_{i=1}^{N} k_i \exp(p_i t)u(t) \tag{9}$$

Here $\delta(t)$ represents a Dirac delta function, not skin depth, and $u(t)$ denotes the unit step function. The quantities k_i are residues and the p_i are poles. In general both are complex. In order for the above rational function to provide physically meaningful results for a passive system (such as a metal interconnect), it is necessary for the poles to have negative real parts. Otherwise the exponentials grow without bound. The impulse response in (9) is clearly causal because the unit step function is zero for $t < 0$.

In practice the rational function fitting is implemented by a least-squares procedure that tries to minimize the difference between the original frequency response data (sampled at a finite set of discrete frequencies) and the model response. It does this by making appropriate choices of the poles and residues. Methods for rational fitting include vector fitting [6], techniques based upon Löwner matrices [7], and many others.

Non-causal input data presents a serious problem for these methods[2]. Because the basis of the model is a set of causal functions, any non-causal components in the input data can never be fitted exactly by them. Depending on the severity of the non-causality, the fitting process may either fail completely, or the obtainable fitting accuracy may be severely limited. The main goal of having an improved surface roughness model is greater accuracy, so if we are unable to accurately fit the resulting data this is a serious problem. We now turn to a proposed remedy for the non-causality problem.

Correcting the Causality Problem

The problem with the real-valued Huray roughness factor $H_r(j\omega)$ is that it is not causal. As we have seen, causality is not possible for a real-valued function of frequency. Therefore we now introduce a complex-valued Huray factor $H_c(j\omega)$, and we assume that the surface impedance for the rough surface can then be calculated as

$$Z_{rough}(j\omega) = Z_s(j\omega) \cdot H_c(j\omega) \tag{10}$$

Now using the smooth surface impedance from (2), the impedance for the rough surface will be

$$Z_{rough}(j\omega) = H_c(j\omega)(1+j)\sqrt{\frac{\omega\mu}{2\sigma}}$$

The real part of $Z_{rough}(j\omega)$ (which governs the measured power losses) is

[2] It is also a problem for methods based on the inverse FFT and convolution, because the non-causality then shows up as spurious, long-delayed spikes in the impulse response.

$$\mathrm{Re}[Z_{rough}(j\omega)] = \{\mathrm{Re}[H_c(j\omega)] - \mathrm{Im}[H_c(j\omega)]\}\sqrt{\frac{\omega\mu}{2\sigma}} \tag{11}$$

If we had used the original real-valued Huray factor, the corresponding prediction for the real part of the surface impedance would have been

$$\mathrm{Re}[H_r(\omega)Z_s(j\omega)] = H_r(\omega)\sqrt{\frac{\omega\mu}{2\sigma}} \tag{12}$$

We believe based on results in [4] that the losses from the above formula are accurate, so we want the new formula based on the complex-valued Huray factor to match the above. By comparing (11) and (12), we see that we must have

$$\mathrm{Re}[H_c(j\omega)] - \mathrm{Im}[H_c(j\omega)] = H_r(j\omega) \tag{13}$$

To make the process of identifying a suitable $H_c(j\omega)$ easier, we are going to simplify the notation. We rewrite the real-valued $H_r(j\omega)$ to make its frequency dependence explicit, as follows:

$$H_r(\omega) = 1 + \sum_{i=1}^{n} H_r^{(i)}(j\omega) \tag{14}$$

We have introduced separate transfer functions for each class of nodule:

$$H_r^{(i)}(j\omega) = \frac{K_i}{1 + \left(\frac{\omega}{\omega_i}\right)^{-\frac{1}{2}} + \frac{1}{2}\left(\frac{\omega}{\omega_i}\right)^{-1}} \tag{15}$$

Here the derived quantities K_i and ω_i are

$$K_i = \frac{6\pi a_i^2 N_i}{A_{hex}} \tag{16}$$

$$\omega_i = \frac{2}{a_i^2 \mu\sigma} \tag{17}$$

We can think of K_i as the maximum increase in the surface loss due to the i^{th} class of nodule. ω_i is an associated "corner" frequency, essentially the frequency where the skin depth becomes equal to the nodule radius a_i. As shown in Figure 2 below, for frequencies well below the corner frequency, $H_r^{(i)}$ goes quickly to zero. For frequencies well above the corner frequency, it approaches K_i.

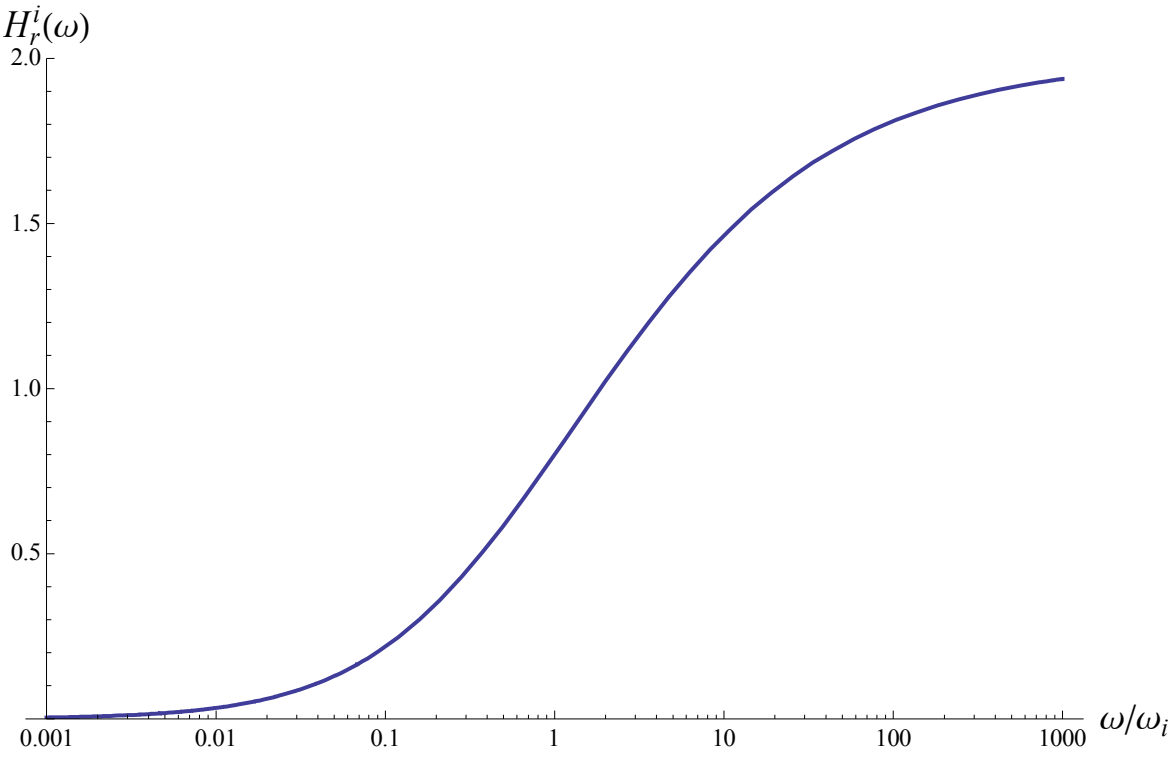

Figure 2. An example of the behavior of the real-valued transfer function $H_r^{(i)}(\omega)$ as a function of frequency, for $K_i = 2$.

Now for the main result of this work: we can show using simple mathematics (see the Appendix) that the following complex-valued Huray factor satisfies (13) *exactly:*

$$H_c(\omega) = 1 + \sum_{i=1}^{n} H_c^{(i)}(j\omega) \tag{18}$$

Here we define

$$H_c^{(i)}(j\omega) = \frac{K_i}{1 + \left(\frac{j2\omega}{\omega_i}\right)^{-1/2}} \tag{19}$$

Figure 3 below provides a comparison of $\mathrm{Re}\left[H_c^{(i)}(j\omega)\right] - \mathrm{Im}\left[H_c^{(i)}(j\omega)\right]$ versus $H_r^{(i)}(j\omega)$ for $K_i = 2$. This shows that the losses are identical with those of the original real-valued Huray model.

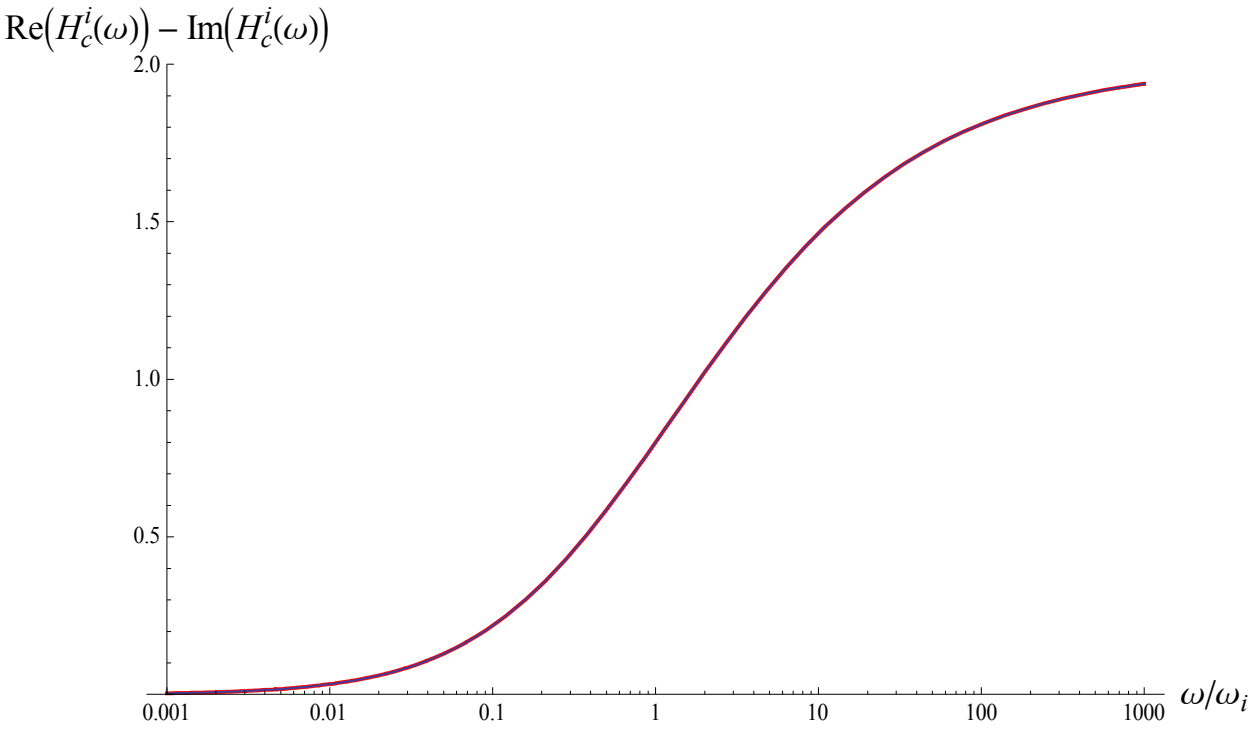

Figure 3. Comparison of the surface loss increases predicted by the complex-valued Huray model (red) with those of the real-valued Huray model (blue). This is shown for the case $K_i = 2$.

It still remains to demonstrate that we have actually corrected the causality problem. Fortunately, we can show that the individual $H_c^{(i)}(j\omega)$ terms of (18) are causal by taking their analytic inverse Laplace transforms. From results in [8] the impulse response is calculated to be

$$h_c^{(i)}(t) = K_i\delta(t) - K_i\widehat{\omega}_i\left[\frac{1}{\sqrt{\pi\widehat{\omega}_i t}} - e^{\widehat{\omega}_i t}\,\mathrm{erfc}\left(\sqrt{\widehat{\omega}_i t}\right)\right]u(t) \qquad (20)$$

Here we defined $\widehat{\omega}_i = \omega_i/2$, and erfc() is the complementary error function. The above function is completely causal because it is zero for $t < 0$. It is difficult to plot the impulse response due to the Dirac delta function, so we instead plot the corresponding unit step response in Figure 4. As the figure shows, the response is indeed causal.

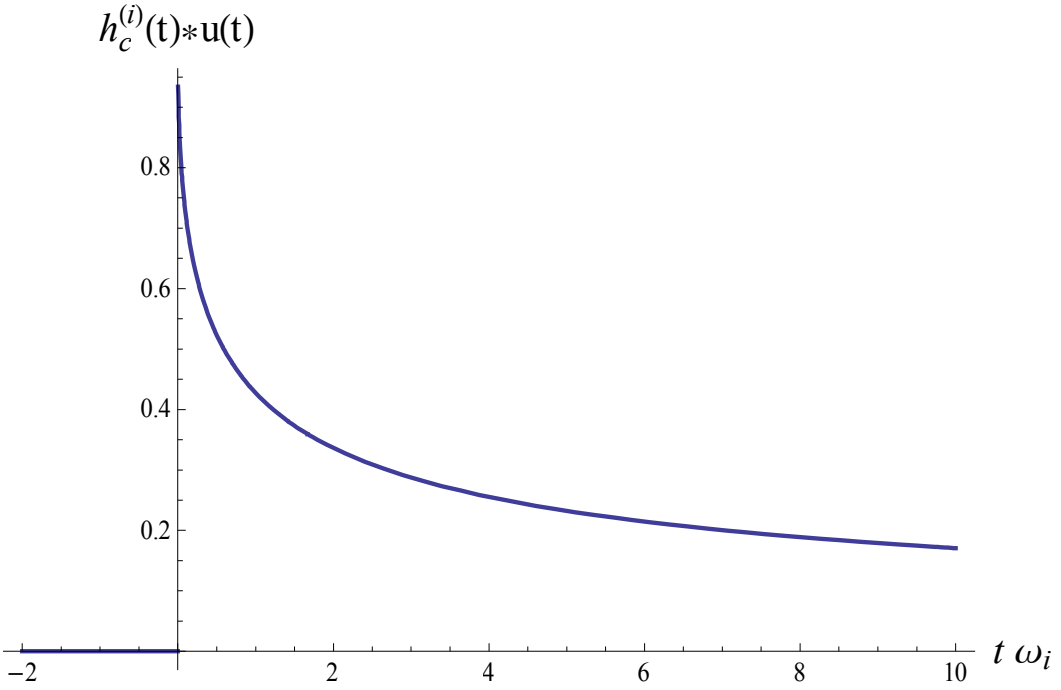

Figure 4. Step response of the complex causal Huray function. Note the response is zero for t < 0. Also note that time has been normalized by multiplying it by $\hat{\omega}_i$ and the vertical scale has been normalized by assuming $K_i = 1$.

Numerical Experiments

The authors of [9] have performed measurements of microstrip transmission lines in low and high profile (i.e. high roughness) copper. We compare their measurement data with the predictions of our new IBC based upon the complex roughness factor of Eq. (19) combined with the finite-thickness model of Eq. (4). Figure 5 below illustrates the excellent agreement of the causal IBC model with measurement. Here we used a single type of sphere with radius $a = 0.5$ um, $N = 72$ and $A_{hex} = 100$ um^2. We have used causal Djordjevic-Sarkar dielectric models [10] for the substrate (2.56 mils thick, $\epsilon_r = 3.78$, $\tan\delta = 0.0086$ at 7 GHz) and solder mask (1.59 mils thick, $\epsilon_r = 3.5$, $\tan\delta = 0.025$ at 7 GHz.) Also shown is the result using the non-causal real-valued model.

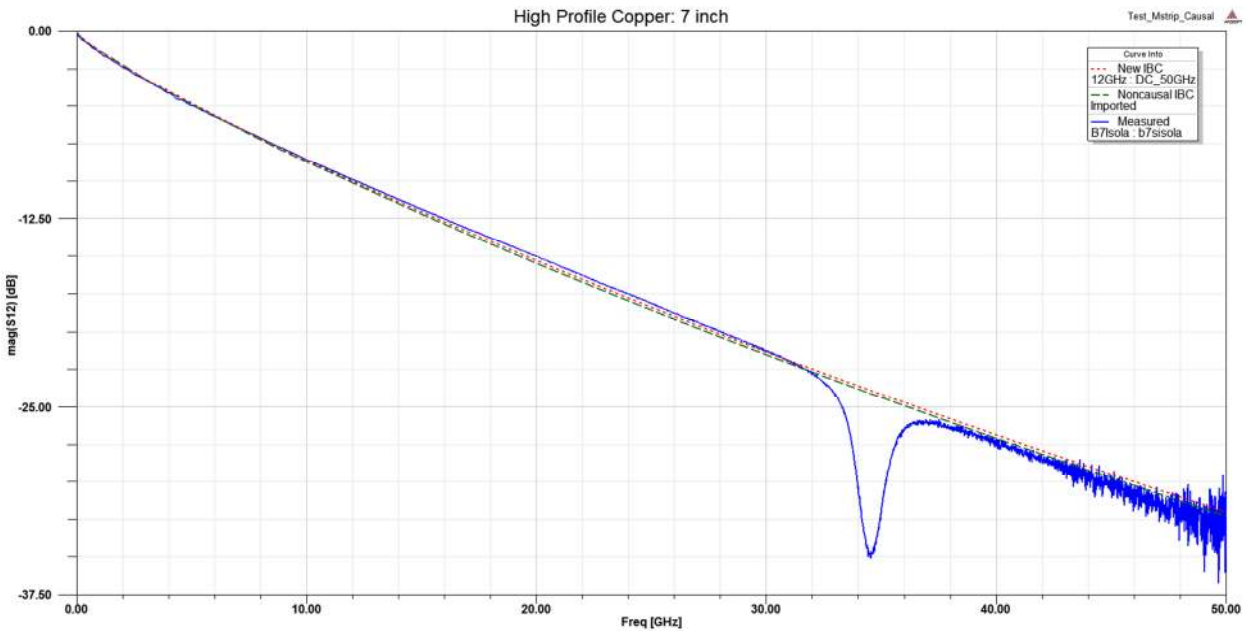

Figure 5. Comparison of causal IBC insertion loss results (red, short dashed) with measurement (blue, solid line) and non-causal IBC (green, long dashed) for 7-inch microstrip trace using high profile copper foil.

From the insertion loss results in Figure 5, there does not appear to be a big difference between the causal and non-causal IBC's. This is because the plots consider only the magnitude of the frequency response. If we examine the phase delay (defined as the unwrapped phase of S12 divided by the angular frequency) as shown in Figure 6 below, we can see a greater difference. The causal IBC produces a result which follows the measurement data much more closely than the non-causal IBC.

Next we consider the time-domain behavior of the S-parameter data. We extracted two sets of S-parameters: the first used the real-valued Huray factor as a multiplier for the finite-thickness impedance boundary condition and the second used the complex-valued Huray factor of Eq. (19) as the multiplier. We performed rational function fitting on the data using a target error tolerance of 0.001. On the first (non-causal) data set, the best obtainable model had a fitting error of 0.0029, or approximately 3 times higher than requested, and used 472 poles. On the second data set (generated by the causal IBC), the fitting error obtained is 0.000997, meeting the requested tolerance. The number of poles used was also lower: 348.

We then ran transient simulations of the two models. We used a Thévenin-equivalent linear driver with 0.5 Ω series resistance, and a linear 200 ps ramp from 0 to 1 Volt; the load was a 50 Ω lumped resistor. The resulting far-end waveforms are shown in Figure 7 below. The causal IBC produces a realistic waveform, whereas the IBC based on the real-valued Huray model has a noticeable non-physical "precursor" before the signal arrives at approximately 1.05 ns.

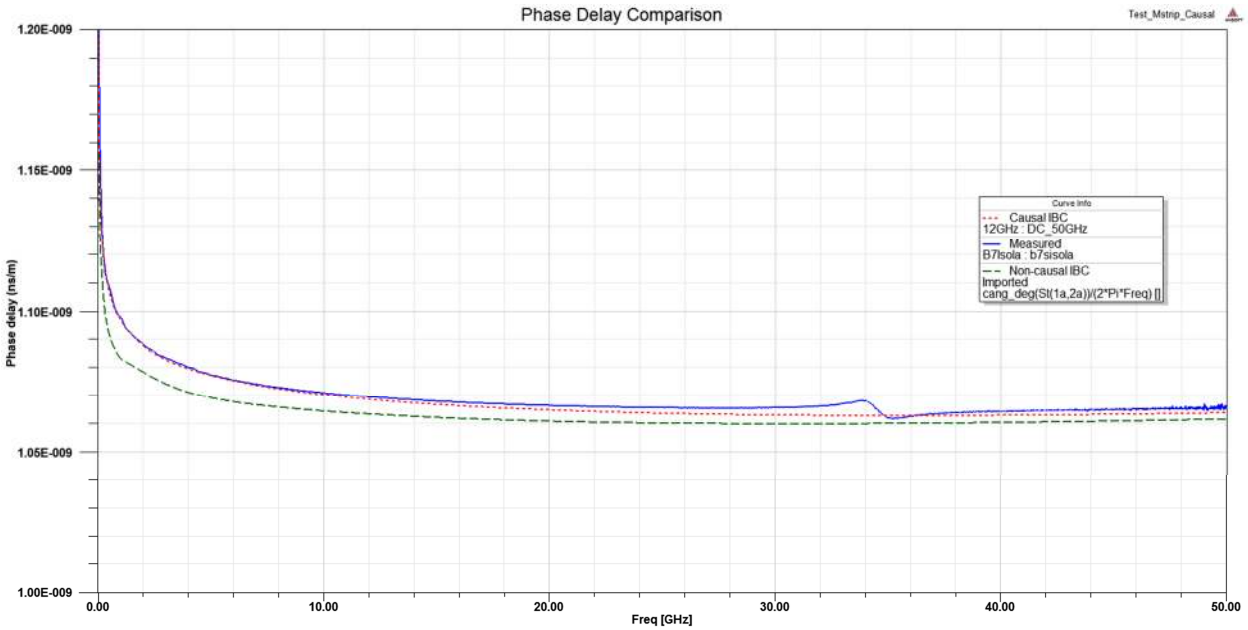

Figure 6. Comparison of phase delay for the causal IBC (red, short dashed) with measurement (blue, solid) and the non-causal IBC (green, long dashed) for 7-inch microstrip trace in high profile copper foil.

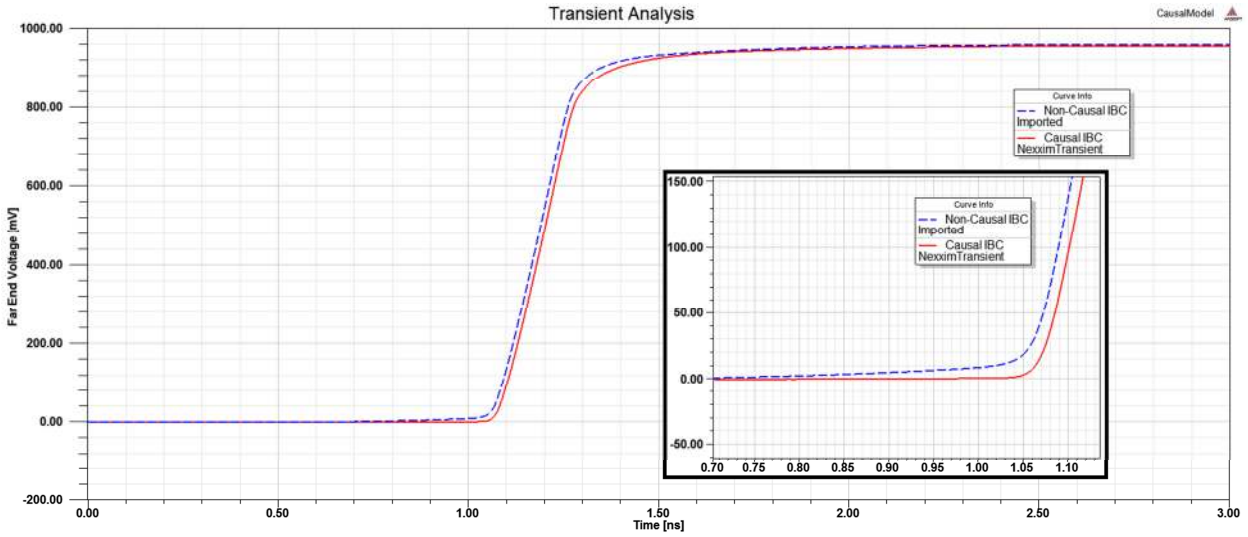

Figure 7. Comparison of the transient responses at the far end of the 7-inch microstrip lines using the causal IBC (red, solid) and the non-causal IBC (blue, dashed.) The inset shows a zoomed-in view of the non-physical precursor predicted by the non-causal IBC.

Conclusion

This paper has presented a modification to the surface roughness model proposed originally by Huray *et al.* to make it useful for implementation as an impedance boundary condition in an electromagnetic field solver. Particular attention was paid to making the resulting impedance boundary function causal so that it can be used as the basis for time domain simulations. Numerical results show that the new IBC does indeed provide improved time-domain behavior.

Bibliography

[1] E. Hammerstad and O. Jensen, "Accurate Models for Microstrip Computer-Aided Design," in *IEEE MTT-S Intl. Microwave Symposium Digest*, Washington, DC, 1980.

[2] S. Groiss, I. Bardi, O. Biro, K. Preis and K. R. Richter, "Parameters of lossy cavity resonators calculated by the finite element method," *IEEE Trans. on Magnetics,* vol. 32, no. 3, pp. 894-897, 1996.

[3] S. Hall, S. G. Pytel, P. G. Huray, D. Hua, A. Moonshiram, G. A. Brist and E. Sijercic, "Multigigahertz Causal Transmission Line Modeling Methodology Using a 3-D Hemispherical Surface Roughness Approach," *IEEE Trans. on Microwave Theory and Techniques,* vol. 55, no. 12, pp. 2614-2624, 2007.

[4] P. G. Huray, O. Oluwafemi, J. Loyer, E. Bogatin and X. Ye, "Impact of Copper Surface Texture on Loss: A Model that Works," in *DesignCon 2010 Proceedings*, Santa Clara, CA, 2010.

[5] A. V. Oppenheim, A. S. Willsky and S. Hamid, Signals and Systems (2nd ed.), Englewood Cliffs, NJ: Prentice Hall, 1996.

[6] B. Gustavsen and A. Semlyen, "Rational approximation of frequency domain responses by vector fitting," *IEEE Trans. on Power Delivery,* vol. 14, no. 3, pp. 1056-1061, 1999.

[7] S. Lefteriu and A. C. Antoulas, "A New Approach to Modeling Multiport Systems From Frequency-Domain Data," *IEEE Trans. on Computer-Aided Design of Integrated Circuits and Systems,* vol. 29, no. 1, pp. 14-27, 2010.

[8] M. Abramowitz and I. A. Stegun, Handbook of Mathematical Functions: with Formulas, Graphs, and Mathematical Tables, Washington, DC: U.S. Dept. of Commerce, National Bureau of Standard, 1964.

[9] S. G. Pytel, P. G. Huray, S. H. Hall, R. I. Mellitz and G. Brist, "Analysis of copper treatments and the effects on signal propagation," in *Electronic Components and Technology Conference*, Lake Buena Vista, FL , 2008.

[10] A. R. Djordjevic, R. M. Biljic, V. D. Likar-Smiljanic and T. K. Sarkar, "Wideband Frequency-Domain Characterization of FR-4 and Time-Domain Causality," *IEEE Trans. on Electromagnetic Compatibility,* vol. 43, no. 4, pp. 662-667, 2001.

Appendix: Equivalence of the Losses in the Complex and Real-Valued Models

Start with

$$H_c^{(i)}(j\omega) = \frac{K_i}{1 + \left(\frac{j2\omega}{\omega_i}\right)^{-1/2}}$$

Rewrite this as

$$H_c^{(i)}(j\omega) = \frac{K_i}{1 + \frac{1}{1+j}\left(\frac{\omega}{\omega_i}\right)^{-\frac{1}{2}}} = K_i \frac{(1+j)}{1 + \left(\frac{\omega}{\omega_i}\right)^{-\frac{1}{2}} + j}$$

Clearing complex variables from the denominator yields

$$H_c^{(i)}(j\omega) = K_i \frac{(1+j)\left\{1 + \left(\frac{\omega}{\omega_i}\right)^{-\frac{1}{2}} - j\right\}}{2 + 2\left(\frac{\omega}{\omega_i}\right)^{-\frac{1}{2}} + \left(\frac{\omega}{\omega_i}\right)^{-1}}$$

This simplifies to

$$H_c^{(i)}(j\omega) = K_i \frac{2 + \left(\frac{\omega}{\omega_i}\right)^{-\frac{1}{2}} + j\left(\frac{\omega}{\omega_i}\right)^{-\frac{1}{2}}}{2 + 2\left(\frac{\omega}{\omega_i}\right)^{-\frac{1}{2}} + \left(\frac{\omega}{\omega_i}\right)^{-1}}$$

Finally, taking the real part minus the imaginary part gives

$$\mathrm{Re}\left[H_c^{(i)}(j\omega)\right] - \mathrm{Im}\left[H_c^{(i)}(j\omega)\right] = K_i \frac{2}{2 + 2\left(\frac{\omega}{\omega_i}\right)^{-\frac{1}{2}} + \left(\frac{\omega}{\omega_i}\right)^{-1}} = \frac{K_i}{1 + \left(\frac{\omega}{\omega_i}\right)^{-\frac{1}{2}} + \frac{1}{2}\left(\frac{\omega}{\omega_i}\right)^{-1}}$$

This is the same as the real-valued Huray factor $H_r^{(i)}(j\omega)$ in (15).